Optical Engineering

OpticalEngineering.SPIEDigitalLibrary.org

Engineering the dispersion properties of multilayered periodic segmented waveguides and nanowire waveguides

Ana Julia R. F. de Oliveira
Vitaly F. Rodriguez-Esquerre
Zhaowei Liu

SPIE.

Ana Julia R. F. de Oliveira, Vitaly F. Rodriguez-Esquerre, Zhaowei Liu, "Engineering the dispersion properties of multilayered periodic segmented waveguides and nanowire waveguides," *Opt. Eng.* **58**(9), 097107 (2019), doi: 10.1117/1.OE.58.9.097107.

Engineering the dispersion properties of multilayered periodic segmented waveguides and nanowire waveguides

Ana Julia R. F. de Oliveira,[a] Vitaly F. Rodriguez-Esquerre,[b,*] and Zhaowei Liu[c]
[a]Federal University of Vale São Francisco, Computer Engineering Collegiate, Petrolina, Brazil
[b]Federal University of Bahia, Department of Electrical Engineering and the Graduate School of Electrical Engineering, Bahia, Brazil
[c]University of California, Electrical and Computer Engineering Department, San Diego, California, United States

Abstract. We proposed and systematically analyzed the propagation properties of periodic segmented waveguides and nanowire waveguides where the segments and nanowires have been considered to be composed of multilayers of silicon and silica with subwavelength thickness. We demonstrated, through a comprehensive number of numerical simulations involving modal analysis, that the artificial uniaxial negative anisotropy introduced by the multilayered segments or nanowire can be used to engineer waveguides with independent polarization propagation characteristic over the entire band of optical communication frequencies. [DOI: 10.1117/1.OE.58.9.097107]

Keywords: waveguides; metamaterials; dispersion; polarization.

Paper 190623 received May 9, 2019; accepted for publication Aug. 27, 2019; published online Sep. 17, 2019.

1 Introduction

Optical waveguides are the main components of any integrated optical circuit, and they have the ability to confine the light by total internal reflection as occurs in usual dielectric waveguides[1,2] or by exploiting the forbidden band gaps as in photonic crystal waveguides.[3,4] Nowadays, many applications are sensitive to light polarization and require polarization maintaining components and waveguides with low losses and high confinement of the light.[5] High index-contrast dielectric waveguides can confine the light in small regions and reduce the radiation losses present in sharp bends. However, they exhibit polarization sensitivity and roughness losses.[2] To reduce the roughness losses and to control the dispersion properties of dielectric waveguides, the periodic segmented waveguide (PSW) with subwavelength segment length as a guiding device was introduced in Ref. 6. It has been analyzed in detail in Refs. 7–10. Initially, PSWs were used as Bragg gratings to design filters and resonators.[11] It has been demonstrated that they can guide light with low losses when the periodicity along the propagating direction is much smaller than the operating wavelength[9] even in the presence of sharp bends,[9] offering a promising platform for designing high-performance waveguide network. PSWs have been considered for the design of directional couplers,[12–14] multimode interferometers,[15,16] crossing with low cross talk,[17] and also in the design of tapers to match the mode of the input source with the desired mode of conventional waveguides.[18] In addition, a type of waveguide structure called nanowire waveguide (NW) has been introduced and analyzed in detail in Ref. 19. They also present high polarization dependence and low bending losses.[20] They have been used to design bends,[20] directional couplers,[13,14] multimode interferometers,[16] and electrically tunable crystal liquid PSW.[21] Consequently, PSWs and NWs are expected to enable ultrasmall and highly functional photonic devices to be developed.

One of the main characteristics of the PSWs and NWs is their high polarization-dependent operation since the dispersion curves of the transversal electric (TE) and transversal magnetic (TM) modes exhibit stop bands at different frequencies.[6–10,22] In general, PSWs and NWs can propagate TE polarized light at higher frequencies than TM polarized waves.[6–10,22] The large polarization dependency can be an important issue depending on the type of application, for example, the coupling distances in directional couplers and multimode interferometers based on PSWs and NWs are different depending on the polarization.[12–14,16]

Recently, there has been an effort to obtain polarization-independent waveguides.[21,23–26] The most trivial way to create polarization-independent waveguides is to design waveguides with vertical and horizontal symmetries, i.e., optical fibers, where the modes will become degenerated. Another approach is to adjust the core width and the etch depth in a rib waveguide, as presented in Refs. 21, 23, and 24. Moreover, polarization-independent waveguiding in photonic crystals have been also reported in Refs. 25 and 26. It is possible to obtain degenerated modes inside the band gap by combining two layers of photonics crystals with rods and holes[25] and also by using annular elements,[26] respectively.

The birefringence has been largely explored in order to design optical devices.[27,28] Taking advantage of this effect, silicon and liquid crystal subwavelength gratings (SWG) waveguides have demonstrated a still better behavior,[21,29] compared to dielectric waveguides. For example, compact polarization beam splitters have been manufactured with dimensions <100 μm,[29] obtaining insertion losses about 2 dB for both polarizations covering the entire C band. In addition, the degree of the birefringence can be tailored only by changing SWG's structural parameters such as the grating

*Address all correspondence to Vitaly F. Rodriguez-Esquerre, E-mail: vitaly.esquerre@ufba.br

0091-3286/2019/$28.00 © 2019 SPIE

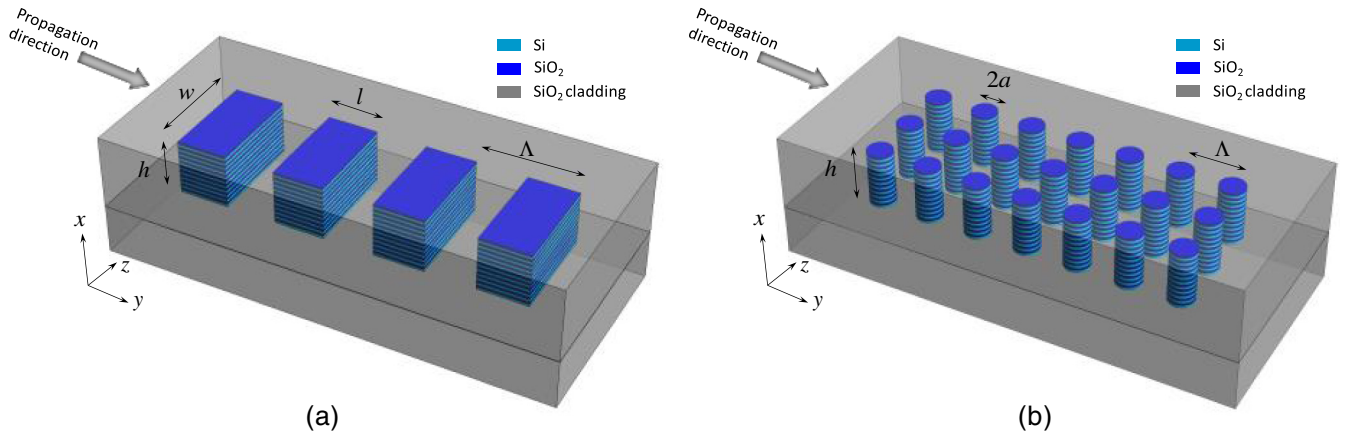

Fig. 1 (a) Proposed multilayered PSW and (b) multilayered nanorod waveguide. The segments and nanorods consist of several layers of silicon/silica with deep-subwavelength thickness cladded by SiO_2.

period, the fill factor, and the grating depth.[30] The manipulation of birefringence through modifications in the physical parameters of the SWG allows the development of some optical devices for the silicon-on-insulator platform as MMI couplers and polarization beam splitters.[29]

In this work, we demonstrated through a comprehensive number of numerical simulations involving modal analysis, that the artificial uniaxial negative anisotropy introduced by a multilayered superlattice can be used to design polarization-independent PSWs and NWs over the entire band of optical communication frequencies. To the best of our knowledge, this is the first time that polarization-insensitive propagation has been reported for PSWs and NWs.

This work is organized as follows. In Sec. 2, a brief description of the PSW and NW and their polarization dependence are given. Also in Sec. 2, the proposed geometry and the uniaxial anisotropy introduced by the subwavelength nature of the multilayer is presented. Numerical results are presented in Sec. 3 and the main conclusions are summarized in Sec. 4.

2 Artificial Anisotropy

To overcome the intrinsic polarization dependence of PSWs and NWs, we propose a new geometry of PSWs and NWs where the segments or nanowires are composed of multilayers of dielectric materials, namely silicon and silica, as shown in Fig. 1.

We consider this composition because of the feasibility of fabrication with thicknesses in the order of few nanometers,[31–36] which is much smaller than the operating wavelength to be considered. Because of the subwavelength size of the thickness silicon and silica layers, the homogenization theory[37] can be applied, and consequently the equivalent homogeneous material exhibits uniaxial negative anisotropy (Fig. 2), with its extraordinary refractive index lower than the ordinary one, $n_e < n_o$, satisfying in this way, one of the needed condition for the proposed polarization-independent PSW. Conventional waveguides composed of silicon nanocrystal superlattice at visible frequencies have been investigated in Ref. 35, and it has been demonstrated that if the core of a planar waveguide is composed of subwavelength thickness layers that will show birefringence.[35,36]

According to the homogenization theory, the equivalent permittivity can be obtained by Ref. 37.

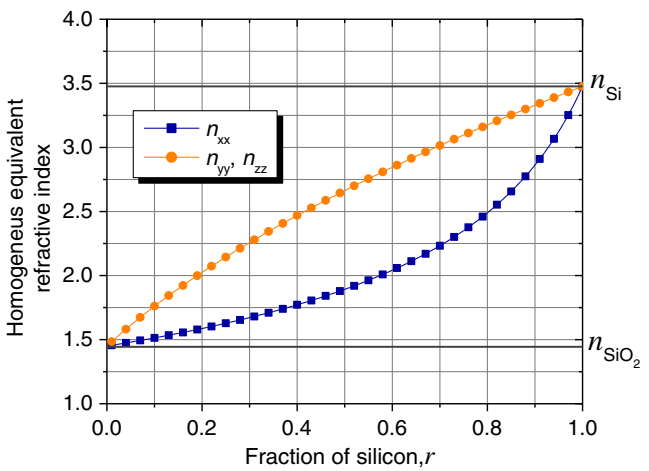

Fig. 2 Homogeneous equivalent anisotropic refractive indices of the multilayer silicon/silica as a function of silicon fraction.

$$\varepsilon_{\perp} = \varepsilon_{xx} = \frac{\varepsilon_1 \varepsilon_2}{(1-r)\varepsilon_1 + r\varepsilon_2}, \tag{1}$$

$$\varepsilon_{||} = \varepsilon_{yy} = \varepsilon_{zz} = (1-r)\varepsilon_2 + r\varepsilon_1, \tag{2}$$

where r is the ratio of silicon on the multilayered segment, with permittivity ε_1 and ε_2 is the permittivity of SiO_2. The refractive indices of silicon and silica considered in this work are 3.476 and 1.45, respectively. For the present analysis, the material dispersion can be neglected since the variation of the refractive indices is small in the *O-E-S-C-L-U* bands (179 to 234 THz). The ordinary and extraordinary refractive indices of the silicon/silica multilayer can be obtained using (1, 2) and the relation $n = \varepsilon^{1/2}$. The obtained values are shown in Fig. 2.

By considering that the surrounding material is all silica and also under the approximation that the height of the segments is larger than the operating wavelength,[36] a two-dimensional (2-D) modal analysis can be carried out by using the efficient frequency domain finite element approach presented in Ref. 9, in order to obtain the dispersion curves of the waveguide. The resulting 2-D waveguide is shown in Fig. 3.

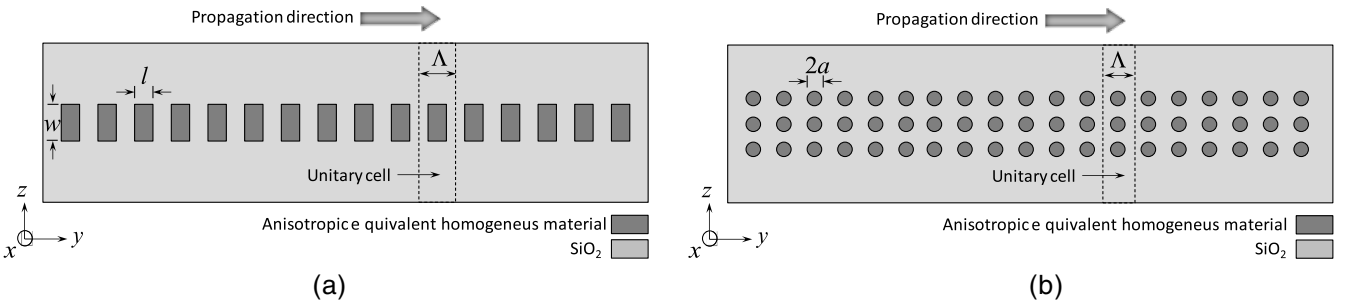

Fig. 3 The 2-D approximation of the (a) PSW and (b) NW, composed of multilayered dielectric segments.

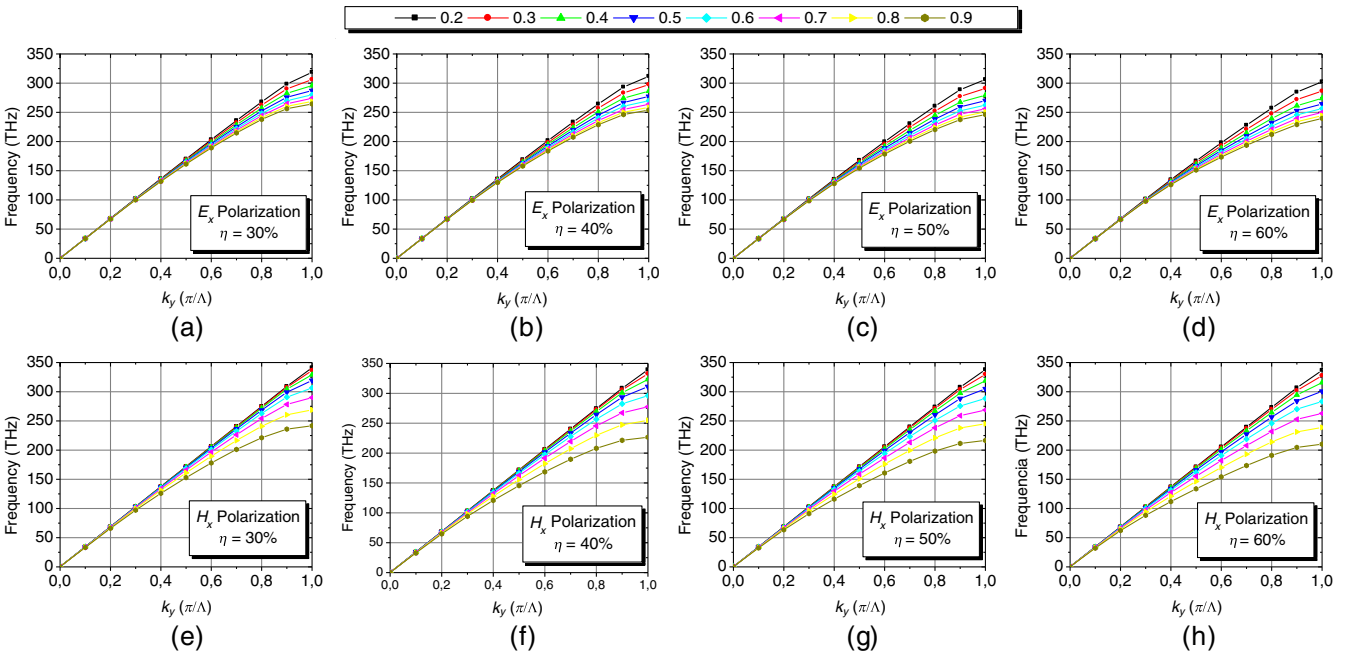

Fig. 4 PSW's dispersion corresponding to silicon ratios on the multilayer from 0.2 to 0.9, polarization and the duty cycle.

3 Numerical Results Style

3.1 *Periodic Segmented Waveguides*

First, we considered a PSW composed of multilayers of silicon and silica. The waveguide parameters are as follows: period and width of 300 nm; a variable duty cycle, $\eta = l/\Lambda$, of 30%, 40%, 50%, and 60%; and the ratio of silicon/silica in the multilayered region has been swept from 0.2 to 0.9. The computational domain corresponding to a unit cell extends from -2 to $+2$ μm and from $-\Lambda/2$ to $+\Lambda/2$ nm in the z and y directions, respectively. Periodical boundary conditions of Bloch type are applied at $z = \pm\Lambda/2$. Considering k_y the wave propagation constant, the resulting dispersion curves as a function of the polarization and duty cycle are shown in Fig. 4.

It can be observed that the highest operating frequency for the H_x polarization as a function of the silicon fraction lies in an interval wider than the ones of the E_x polarization and it also contains those frequencies. The intervals containing the maximum operating frequencies as a function of the duty cycle r and the polarization are given in Table 1.

In Fig. 4, it can be observed that for the proposed multilayered PSW, with duty cycles between 0.3 and 0.6, there is always a specific value of r where the dispersion curves for both polarizations can exhibit a good overlapping and the

Table 1 Maximum operating frequencies as functions of the polarization and the silicon ratio.

Duty cycle	Polarization	f_{min} (THz) ($r = 0.9$)	f_{max} (THz) ($r = 0.2$)
$\eta = 30\%$	E_x	264.31	318.69
	H_x	241.67	341.23
$\eta = 40\%$	E_x	253.98	311.64
	H_x	226.56	339.45
$\eta = 50\%$	E_x	246.19	306.31
	H_x	216.63	337.89
$\eta = 60\%$	E_x	239.66	302.46
	H_x	210.23	336.76

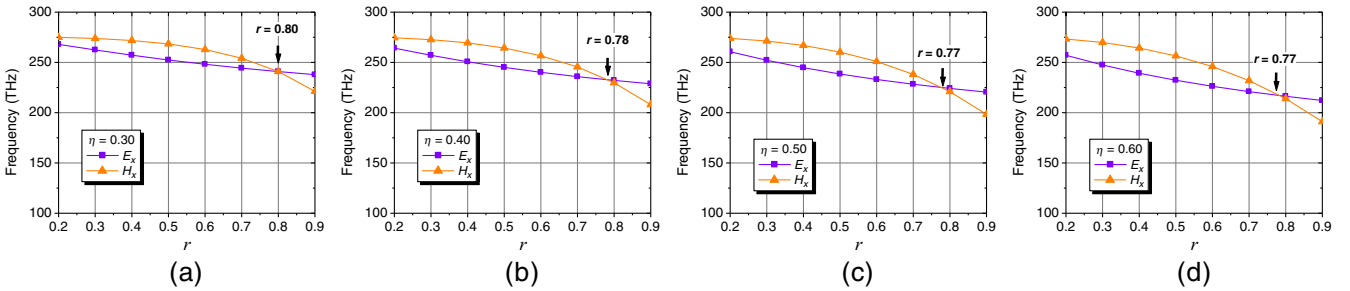

Fig. 5 Frequency of operation of the PSW as a function of r, considering a fixed value of $k_y = 0.8\ \pi/\Lambda$. The value of r indicated corresponds to the condition where both polarizations exhibit the same propagation constant for a given frequency of operation.

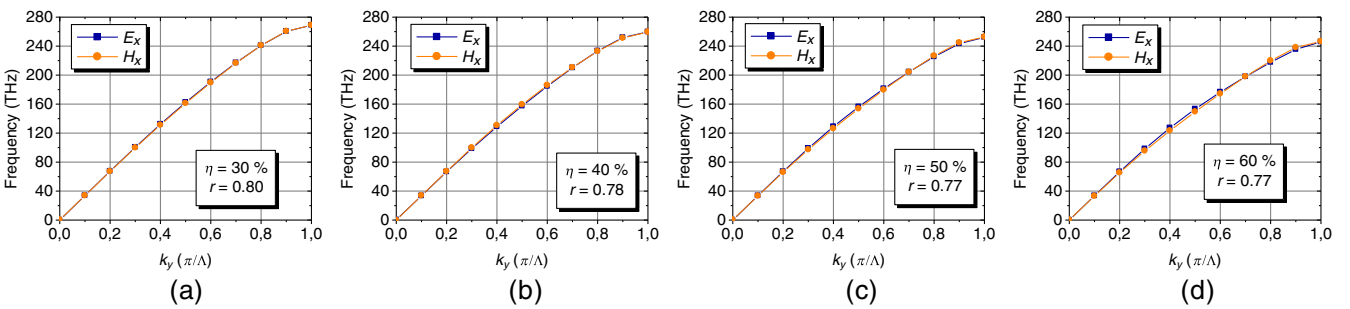

Fig. 6 PSW's dispersion curves under the polarization-independent condition, corresponding to the duty cycle and fraction of silicon.

PSW will operate under the polarization-independent condition. To obtain the specific value of silicon fraction, we considered, for the sake of simplicity, the frequencies of the H_x and E_x modes for a fixed value of $k_x = 0.8$ as a function of the duty cycle, as shown in Fig. 5. It can be observed that for a duty cycle of 30% and 40%, the overlapping occurs when $r = 0.8$ and $r = 0.78$, respectively [Figs. 5(a) and 5(b)], whereas for duty cycles of 50% and 60%, the value of r where the dispersion curves for both polarization exhibit an overlapping with each other occurs when $r = 0.77$ [Figs. 5(c) and 5(d)].

The dispersion curves for both polarizations, considering the specific value of r, where the overlapping occurs, are shown in Fig. 6. It can be also observed that as the duty cycle increases, the overlapping decreases slightly, mainly, at lower frequencies, but it is still good around 200 THz. The overlap of the dispersion curves for both polarizations is excellent even for larger variations of the duty cyclee of the order of 30%. The necessary ratio of silicon in the multilayer segment changed only 3% t attend the overlapping condition, suggesting that the length of the segment does not influence on the desired behavior much. We also observe a shift in the maximum operating frequencies of both curves as the duty cycle changes.

We also analyzed the influence of the segment width by increasing it to 330 nm for a duty cycle equal to 50%. The results are shown in Fig. 7. Comparing Figs. 7(a) and 7(b) with Figs. 4(c) and 4(g), we can observe a reduction in the frequency values. From Fig. 7(c), we can observe an increment in the optimal filling fraction from 0.77 ($w = 300$ nm) to $r = 0.80$ ($w = 330$ nm), considering as reference $k_y = 0.8\ \pi/\Lambda$. We also present the dispersion curves for both polarizations for $r = 0.80$. The overlapping of the curves is good for values of k_y near $0.8\ \pi/\Lambda$ or frequencies about 210 THz.

In addition, we analyze the influence of the filling fraction on the propagation characteristics of the proposed PSWs by fixing the operating frequency in 200 THz ($\lambda = 1500$ nm). The results are shown in Fig. 8. The variation of the propagation constant as a function of the filling ratio is shown in Fig. 8(a), where the continuous and dashed lines corresponds to E_x and H_x polarization waves, respectively. The polarization-independent operation is obtained for the filling ratio value at the intersection of the same color curves. The difference between the k_y of the E_x and H_x polarized modes has been computed and they are shown in Fig. 8(b). It can be observed from Fig. 8(b) that an increase in the filling ratio results in higher variation of the propagation constant difference, if compared to a decrease in the filling ratio. Also, we can observe less influence of the filling ratio on the propagation constant for low values of duty cycle.

3.2 *Periodic Nanowire Waveguides*

A similar analysis has been carried out for multilayer NWs. The multilayered NW is composed of three parallel rods with variable radii of 80 and 100 nm with their center placed at fixed positions on the plane (y, z): $(\pm m\ \Lambda, -\Lambda)$, $(\pm m\ \Lambda, 0)$, and $(\pm m\ \Lambda, +\Lambda)$, with $m = 0, 1, 2, \ldots$. The period was considered fixed with $\Lambda = 300$ nm (along the propagation direction y), and the ratio of silicon/silica in the multilayered region has been swept from 0.2 to 0.9. The computational domain corresponding to a unit cell, as depicted in Fig. 3(b), extends from -2 to $+2$ μm and from $-\Lambda/2$ to $+\Lambda/2$ nm in the z and y directions, respectively. Periodical boundary

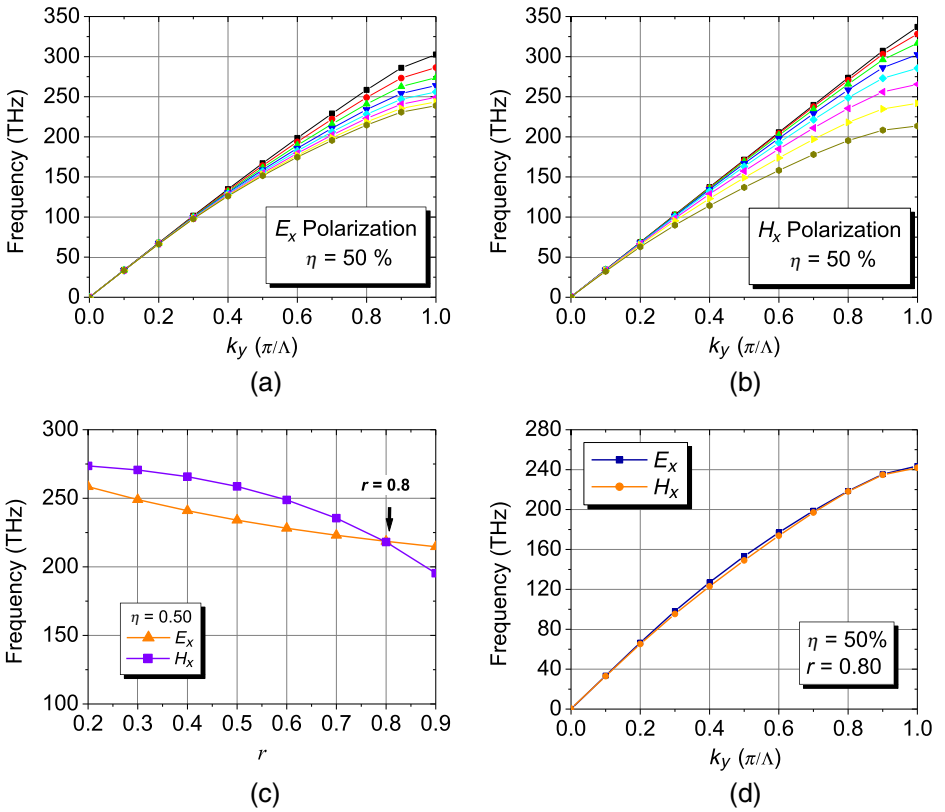

Fig. 7 PSW's dispersion corresponding to silicon ratios on the multilayer from 0.2 to 0.9, polarization with $w = 330$ nm, (a) E_x polarization, (b) H_x polarization, (c) frequency of operation of the PSW as a function of r considering a fixed value of $k_y = 0.8\ \pi/\Lambda$, and (d) dispersion curves under the polarization-independent condition.

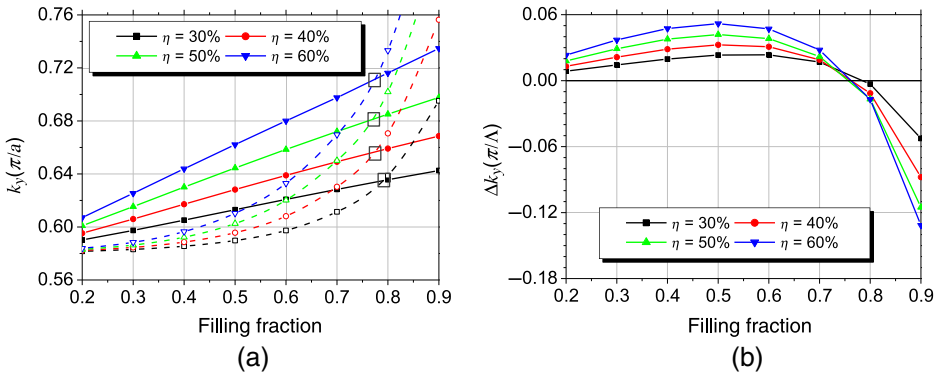

Fig. 8 (a) Dependence of the propagation constant of the E_x and H_x polarized waves with the filling ratio and (b) difference of the propagation constant of the E_x and H_x polarized waves as a function of the filling ratio. $\Lambda = w = 300$ nm.

conditions of Bloch type are applied at $z = \pm\Lambda/2$. The dispersion curves of the NWs for $\Lambda = 300$ nm and $a = 80$ nm and $a = 100$ nm are shown in Fig. 9. It can be observed that the highest operating frequency for the H_x polarization as a function of the silicon fraction lies in an interval wider than the ones of the E_x polarization and it also contains those frequencies. A similar effect has been observed for PSWs.

As expected, there is a value of r where the dispersion curves exhibit an overlapping and its value can be determined considering the frequencies as a function of r with a fixed value of $k_y = 0.8$ (π/Λ). See Fig. 10. It can be observed from Fig. 10(a) that for $r = 0.70$, both polarizations exhibit the same propagation constant for a given frequency for $a = 80$ nm and from Fig. 10(b) both polarizations exhibit the same propagation constant for $r = 0.70$ when $a = 80$ nm. The dispersion curves for both polarizations, considering the polarization-independent condition, are presented in Fig. 11. An excellent overlapping can be observed in all cases.

The filling ratio dependence has been also carried out for the NWs. The results are shown in Fig. 12 and a low

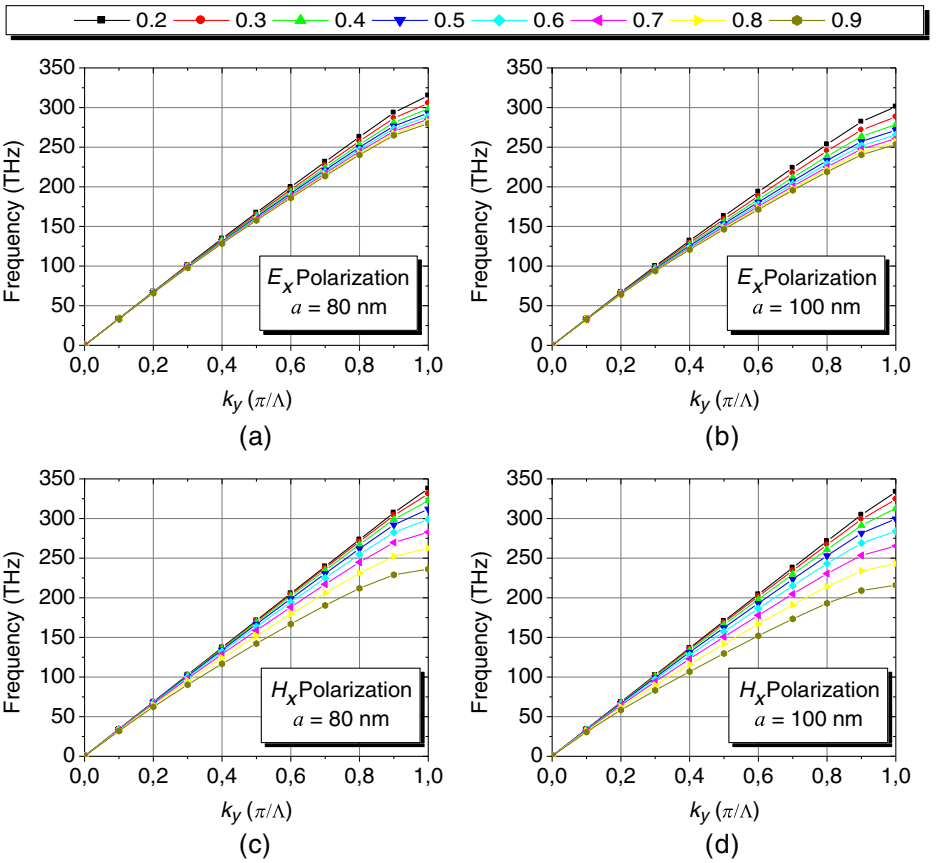

Fig. 9 NW's dispersion curves corresponding to silicon ratios on the multilayer and polarization for $\Lambda = 300$ nm.

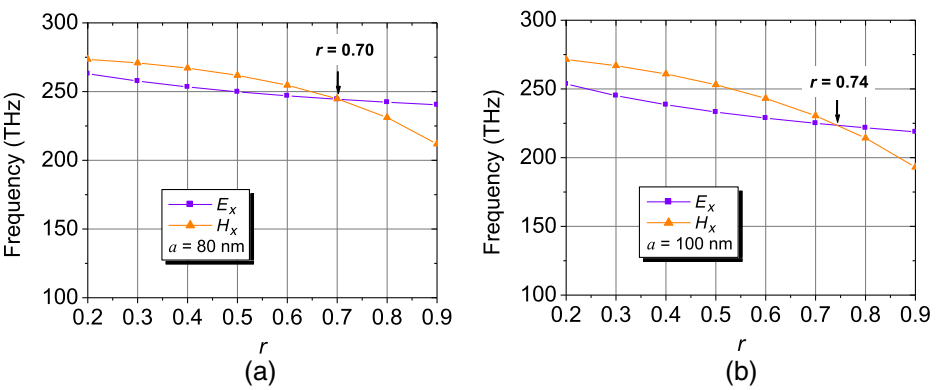

Fig. 10 (a) Frequency of operation of the NWs as a function of r, considering a fixed value of $k_y = 0.8\ \pi/\Lambda$. The value of r indicated corresponds to the condition where both polarizations exhibit the same propagation constant for a given frequency of operation.

influence is observed for nanowires with radius of 100 nm where the propagation constant difference between E_x and H_x polarized waves is about half of the difference for nanowires with radius of 80 nm. It can be observed that both kinds of waveguides, PSWs and NWs, exhibit similar dependence with the filling fraction.

The use of a multilayered segment or multilayered NWs can reduce drastically or eliminate the polarization dependence of PSWs and NWs within a certain interval of frequencies.

The polarization-independent PSWs and NWs, which are analyzed here, are suitable for applications in optical communications, covering the *O-E-S-C-L-U* bands (179 to 234 THz) since the minimum operating wavelength observed in our analysis is 1250 nm ($\eta = 60\%$) [Fig. 6(d)]. Moreover, the proposed strategy exhibits a slight sensitivity with the value of r. Consequently, the proposed strategy to cancel the polarization dependence would be more efficient if we design the waveguide considering the central frequency of operation.

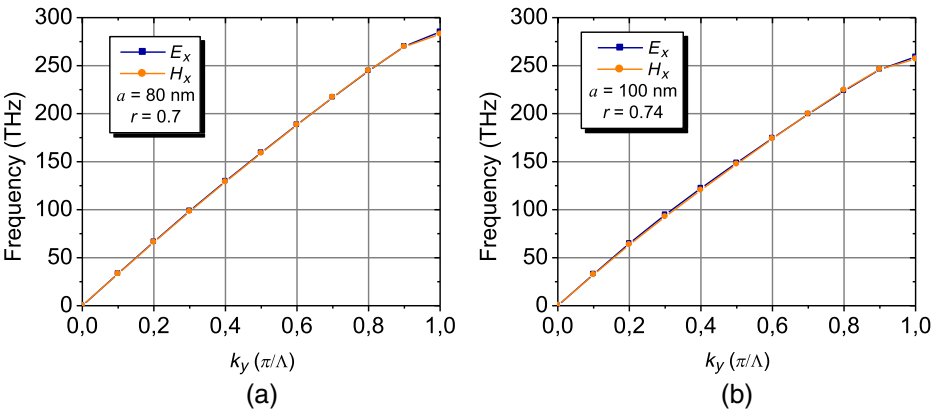

Fig. 11 Dispersion curves of NWs with $\Lambda = 300$ nm under the polarization-independent condition.

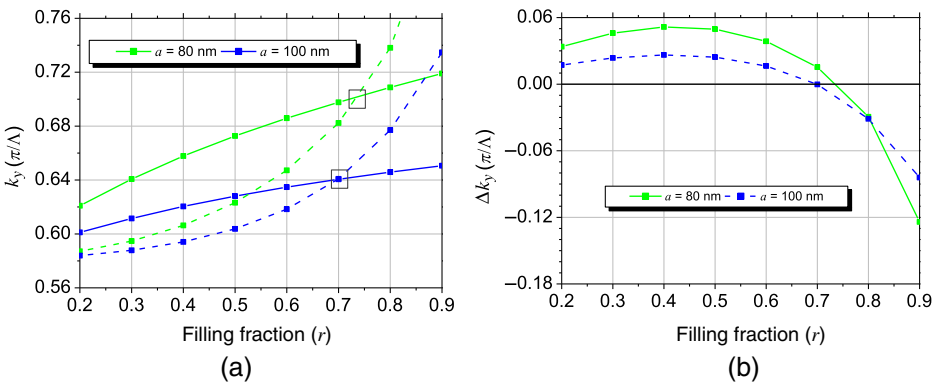

Fig. 12 (a) Dependence of the propagation constant of the E_x and H_x polarized waves with the filling ratio and (b) difference of the propagation constant of the E_x and H_x polarized waves as a function of the filling ratio.

4 Conclusions

As a conclusion, we have proposed and systematically analyzed PSWs and NWs based on subwavelength multilayers with independent polarization propagation properties. We demonstrated through a comprehensive number of numerical simulations involving modal analysis, that the artificial uniaxial negative anisotropy introduced by the multilayered segments and nanowires can be used to engineer waveguides with polarization-independent behavior, and we obtained the necessary design parameters. Our results confirm that, by using multilayered dielectrics composed of Si and SiO_2 with subwavelength thickness, it is possible to reduce drastically or almost cancel the polarization dependence of the propagation characteristics of PSWs and NWs within a certain interval of frequencies. We also observed that for the considered dielectric materials and parameters, the needed value of r for PSWs is about 0.77 to 0.80, depending on the duty cycle, whereas for NWs it is 0.70 to 0.74, depending on the value of the nanowire radius. The proposed strategy can be applied for the design of several polarization-independent devices based on PSWs and NWs such as directional couplers and multimode interferometers.

Acknowledgments

The authors would like to thank CNPq Process 309100/2018-6, CAPES Process 99999.007104/2014-0, UFBA, UNIVASF, and FAPESB (APP 079/2016).

References

1. D. Marcuse, *Theory of Dielectric Optical Waveguides*, Academic Press, Boston (1974).
2. K. Okamoto, *Fundamentals of Optical Waveguides*, Academic Press, Amsterdam (2005).
3. K. Sakoda, *Optical Properties of Photonic Crystals*, Springer, Berlin, Heidelberg (2001).
4. K. Inoue and K. Ohtaka, *Photonic Crystals: Physics, Fabrication and Applications*, Springer Verlag, Berlin, Heidelberg (2004).
5. C. Manolatou et al., "High-density integrated optics," *J. Lightwave Technol.* **17**(9), 1682–1692 (1999).
6. D. Nir et al., "Periodically segmented waveguides in Ti:LiNbO3," *Opt. Lett.* **19**(21), 1732–1734 (1994).
7. D. Ortega, R. M. De La Rue, and J. Stewart Aitchison, "Cutoff wavelength of periodically segmented waveguides in Ti:LiNbO3," *J. Lightwave Technol.* **16**(2), 284–291 (1998).
8. Y. Dong et al., "A theoretical analysis of refractive-index grating waveguide structures for integrated optics," *Opt. Laser Technol.* **39**(4), 1522–1527 (2007).
9. P. J. Bock et al., "Subwavelength grating periodic structures in silicon-on-insulator: a new type of microphotonic waveguide," *Opt. Express* **18**(19), 20251–20262 (2010).
10. A. J. R. F. Oliveira, M. S. Costa, and V. F. Rodriguez-Esquerre, "Propagation characteristics analysis of subwavelength grating waveguides," in *Proc. SBMO/IEEE MTT-S Int. Microwave & Optoelectron. Conf.*, pp. 674–678 (2011).
11. S. M. Hamidi, A. Bananej, and M. M. Tehranchi, "Tunable optical properties in engineered one-dimensional coupled resonator optical waveguides," *Opt. Laser Technol.* **44**(5), 1556–1563 (2012).
12. A. J. R. F. Oliveira et al., "Numerical analysis of periodic segmented waveguides directional couplers," in *Latin America Optics and Photonics Conf.*, paper LM2A.22, OSA Technical Digest, Optical Society of America (2012).
13. L. Uzeda Souza, A. J. R. F. Oliveira, and V. F. Rodriguez Esquerre, "Coupling properties of novel directional couplers composed of silicon nanowires waveguides," in *Latin America Optics and Photonics Conf.*, paper LT1B.5, OSA Technical Digest, Optical Society of America (2012).

14. V. F. Rodriguez-Esquerre et al., "Coupling properties of directional couplers based on special waveguides," *Microwave Opt. Technol. Lett.* **55**(5), 949–951 (2013).
15. A. Maese-Novo et al., "Wavelength independent multimode interference coupler," *Opt. Express* **21**(6), 7033–7040 (2013).
16. A. J. R. F. de Oliveira and V. F. Rodriguez-Esquerre, "Multimode interferometers based on non-conventional waveguides," *Proc. SPIE* **8980**, 89801G (2014).
17. P. J. Bock et al., "Subwavelength grating crossings for silicon wire waveguides," *Opt. Express* **18**(15), 16146–16155 (2010).
18. A. Dourado-Sisnando et al., "Power coupling optimization in 2D waveguides by evolutionary algorithms," *Photonics Technol. Lett.* **27**(14), 1561–1564 (2015).
19. M. Khorasaninejad and S. S. Saini, "Silicon nanowire optical waveguide (SNOW)," *Opt. Express* **18**(22), 23442–23457 (2010).
20. M. Khorasaninejad and S. S. Saini, "Bend waveguides on silicon nanowire optical waveguide (SNOW)," *Photonics J.* **3**(4), 696–702 (2011).
21. M. Sharma, M. R. Shenoy, and A. Sinha, "Periodically-segmented liquid crystal core waveguides," *J. Phys. D: Appl. Phys.* **50**, 385107 (2017).
22. C. E. Rubio-Mercedes et al., "Analysis of straight periodic segmented waveguide using the 2-D finite element method," *J. Lightwave Technol.* **32**(11), 2163–2169 (2014).
23. S. T. Lim et al., "Single mode, polarization-independent submicron silicon waveguides based on geometrical adjustments," *Opt. Express* **15**(18), 11061–11073 (2007).
24. L. Vivien et al., "Polarization-independent single-mode rib waveguides on silicon-on-insulator for telecommunication wavelengths," *Opt. Commun.* **210**(1–2), 43–49 (2002).
25. E. Lidorikis et al., "Polarization-independent linear waveguides in 3D photonic crystals," *Phys. Rev. Lett.* **91**(2), 023902 (2003).
26. A. Cicek and B. Ulug, "Polarization-independent waveguiding with annular photonic crystals," *Opt. Express* **17**(20), 18381–18386 (2009).
27. K. S. Chiang and W. P. Wong, "Design of zero-birefringence semiconductor waveguides," *Proc. SPIE* **3278**, 168–178 (1998)
28. V. M. N. Passaro et al., "Polarization-insensitive directional couplers based on SOI wire waveguides," *Open Opt. J.* **2**, 6–9 (2008).
29. L. Xu et al., "Polarization beam splitter based on MMI coupler with SWG birefringence engineering on SOI," *IEEE Photonics Technol. Lett.* **30**(4), 403–406 (2018)
30. S. Bej et al., "All-optical control of form birefringence," in *Proc. Eur. Conf. Lasers and Electro-Opt.– Eur. Quantum Electron. Conf.*, p. CD_P_16 (2015).
31. W. Peng et al., "Single-crystal silicon/silicon dioxide multilayer heterostructures based on nanomembrane transfer," *Appl. Phys. Lett.* **90**(18), 183107 (2007).
32. E. Agocs et al., "Optical characterization of nanocrystals in silicon rich oxide superlattices and porous silicon," *Thin Solid Films* **519**(9), 3002–3005 (2011).
33. C. Dufour, S. Chausserie, and F. Gourbilleau, "Silicon-rich/silica multilayers: a means to provide a link between the excitonic 1D quantum confinement and the photoluminescence parameters," *J. Lumin.* **129**(1), 73–80 (2009).
34. H. Colder, P. Marie, and F. Gourbilleau, "The silicon-silicon oxide multilayers utilization as intrinsic layer on pin solar cells," *Thin Solid Films* **516**(20), 6930–6933 (2008).
35. F. Riboli et al., "Birefringence in optical waveguides made by silicon nanocrystal superlattices," *Appl. Phys. Lett.* **85**(7), 1268–1270 (2004).
36. P. Cheben et al., "Subwavelength integrated photonics," *Nature* **560**, 565–572 (2018).
37. S. M. Rytov, "Electromagnetic properties of a finely stratified medium," *J. Exp. Theor. Phys.* **2**(3), 466–475 (1956).

Ana Julia R. F. de Oliveira received her BS degree in electrical engineering from the Federal University of Campina Grande, Paraiba, Brazil, in 2010, and her MSc degree and PhD in electrical engineering, from the Federal University of Bahia in 2012 and 2016, respectively. She was at the Interuniversity Microelectronics Centre IMEC (Leuven, Belgium) in 2014 and at the École Nationale Supérieure des Systèmes Avancés et Réseaux France, in 2009. Her current research interest includes numerical methods applied for modal and propagation analysis of electromagnetic fields in nonconventional photonic waveguides and devices.

Vitaly F. Rodriguez-Esquerre received his BS degree in electronic engineering from the University Antenor Orrego, Trujillo, Peru, in 1994, and his MSc degree and PhD in electrical engineering in 1998 and 2003, respectively, from University of Campinas, UNICAMP, Brazil. He was a postdoctoral research fellow at Hokkaido University, Japan, from 2003 until 2005, and he also was a postdoctoral fellow at Unicamp, Brazil, from 2005 until February 2006. He is an associate professor of the ECE at the Federal University of Bahia, UFBA. He was a visiting researcher at the University of California, San Diego (UCSD), in 2015. His current research interest includes numerical methods for modal and propagation analysis of electromagnetic fields in conventional and metamaterial-based integrated optics. He also research evolutionary computing for microwave and optical devices design and computer-assisted learning and education.

Zhaowei Liu (SM'12) received his BS and MS degrees in physics from Nanjing University in 1998 and 2001, respectively. He received his PhD in mechanical engineering (MEMS/nanotechnology) from University of California, Los Angeles, in 2006. He is an associate professor of electrical and computer engineering at UCSD. Before joining the UCSD faculty, he was a postdoctoral researcher at the NSF Nanoscale Science and Engineering Center in the Mechanical Engineering Department at University of California, Berkeley. His current research interest includes nanophotonics, optical imaging, plasmonics, metamaterials, energy, nonlinear optics, and ultrafast optoelectronics.